In HPV-Positive HNSCC Cells, Functional Restoration of the p53/p21 Pathway by Proteasome Inhibitor Bortezomib Does Not Affect Radio- or Chemosensitivity[1,2]

Steve Seltzsam[*,3], Frank Ziemann[*,4], Kristin Dreffke[*], Stefanie Preising[*], Andrea Arenz[*], Ulrike Schötz[*], Rita Engenhart-Cabillic[*], Ekkehard Dikomey[*,†] and Andrea Wittig[*,‡]

[*]Department of Radiotherapy and Radiation Oncology, Philipps University of Marburg, University Hospital Gießen and Marburg, Baldingerstrasse, 35043 Marburg, Germany; [†]Laboratory for Radiobiology & Experimental Radiooncology, University Medical Center Hamburg Eppendorf, Martinistrasse 52, 20246 Hamburg, Germany; [‡]Department of Radiotherapy and Radiation Oncology, University Hospital Jena, Bachstrasse 18, 07743 Jena, Germany

Abstract

Human papillomavirus (HPV) associated squamous cell carcinomas of the head and neck region (HPV+ HNSCCs) harbor diverging biological features as compared to classical noxa-induced (HPV−) HNSCC. One striking difference between subtypes is that the tumor suppressor gene *TP53* is usually not mutated in HPV+ HNSCCs. However, p53 is inhibited by viral oncoprotein E6, leading to premature proteasomal degradation. We asked whether bortezomib (BZM), a clinically approved inhibitor of the proteasome, can functionally restore p53 and investigated in how far this will result in an enhanced radio- or chemosensitivity of HPV+ HNSCC cell lines. For all four HPV+ cell lines tested, BZM led to functional restoration of p53 and transactivation of downstream protein p21. In HPV+ cells, BZM also restored the radiation-induced p53/p21 transactivation. Consistently, in HPV+ cells, a restored G1 arrest as well as enhanced apoptosis were seen when BZM was given prior to irradiation (IR) or cisplatin (CDDP). BZM alone reduced the clonogenic survival of both HPV− and HPV+ cells. However, if BZM was combined with IR or CDDP, BZM did not significantly enhance radio- or chemosensitivity of HPV+ or HPV− HNSCC cell lines.

Translational Oncology (2019) 12, 417–425

Introduction

Squamous cell carcinomas of the head and neck region (HNSCCs) are recognized as two distinct entities with diverging biological features. One entity is induced by classical risk factors like tobacco and alcohol abuse, while the other is associated with high-risk human papillomavirus (HPV) infection [1]. In contrast to a stable incidence for the first entity, the incidence of HPV-associated tumors (HPV+) rises in Europe and the United States [2–4]. This entity is associated with a better response towards simultaneous radiochemotherapy, leading to a better prognosis [5] as compared to HPV negative tumors (HPV–). In spite of these facts, current evidence-based treatment guidelines [6] do not recommend alternative management decisions according to HPV status, which may go along with an overtreatment and preventable side effects in patients with HPV+ HNSCC. Therefore, clinical trials aim to individualize treatment of HNSCC to

avoid side effects without compromising the good response rates of HPV+ HNSCC [7].

The molecular mechanisms leading to the better treatment outcome of HPV+ HNSCC are only partly understood. The main reasons that have been identified so far based on in vitro experiments are an impaired DNA repair capacity and defective cell cycle regulation [8–12] as well as an enhanced induction of p53-dependent apoptosis [13]. Apoptosis might occur in HPV+ HNSCC because these tumors usually harbor the wild-type form of the *TP53* tumor suppressor gene. However, the level of p53 is very low because the viral oncoprotein E6 initiates a premature degradation of p53 by the proteasome [14]. In contrast, in HPV– HNSCC, p53 is mostly mutated [15].

It was already shown for several other tumor entities, that increase of wild-type p53 levels and the restoration of p53-related pathways are both effective and specific strategies to sensitize tumor cells towards antineoplastic drugs [16]. Both strategies can therefore be used for anti-cancer treatments. We investigate here whether in HPV+ HNSCC cells blocking of the proteasomic activity with bortezomib (BZM) lead to a functional restoration of p53 and with that also increase the treatment response of these cells. BZM is an inhibitor of the proteasome that targets the proteolytic subunit leading to reduced protein degradation [17]. It is approved for the treatment of hematopoietic malignancies, leading to good response rates with only few side effects [18].

In HPV+ HNSCC cells, treatment with BZM alone increases p53/p21 expression, resulting in a cell-cycle arrest as well as induction of apoptosis [19,20]. In several studies, BZM was also tested in combination with ionizing irradiation (for overview, see [21]). However, so far, it is unclear whether or not this will lead to an increased radiosensitivity, and data are still lacking for HPV+ HNSCC cells.

We now studied in HPV+ cell lines whether BZM can also be used to restore the p53-dependent functions critical after treatment with ionizing irradiation (IR) or cisplatin (CDDP) and whether this might affect the cellular radio- or chemosensitivity of HNSCC cells. The experiments were performed with four HPV+ HNSCC cell lines and, for control, with four HPV– HNSCC cell lines.

Material and Methods

Cell Lines

Four HPV–, p53-mutated HNSCC cell lines (UM-SCC-3, UM-SCC-11b, UT-SCC-33, UD-SCC-1) and four HPV+, p53 wild-type HNSCC cell lines (UD-SCC-2, UM-SCC-47, UM-SCC-104, UPCI:SCC152) were used. Detailed characteristics of the cell lines and confirmation of HPV status as well as culture conditions have been previously described [8,13,22,23]. Authentication of all cell lines was performed by short tandem repeat analysis at the German Collection of Microorganisms and Cell Cultures (DSMZ, Germany).

Treatment

Bortezomib (BZM; Cell Signaling Technology, Danvers, MA) was diluted in dimethyl sulfoxide (DMSO, stock: 1 mM) according to the manufacturer's instructions and stored at –20°C upon use. Further dilution steps were carried out directly before application, and an equal dilution of DMSO was used as solvent control. Cisplatin (CDDP; TEVA, Ulm, Germany) was supplied as a stock solution (1 mg/ml) (Center for Cytostatics Preparation, University Hospital

Gießen and Marburg, Germany) and further diluted in pure water (stock: 1 mM) directly before application. X-ray irradiation (IR) was carried out using an X-RAD 320 iX (Precision X-Ray Inc., Denver, CO) X-ray tube; anode voltage: 320 kV, current: 10 mA, dose rate: 1.2 Gy/min, focus object distance: 60 cm, filter: 0.5 mm Cu and 0.5 mm Al. Further treatment conditions are indicated in the results section.

Western Blot Analysis

Whole-cell lysates were prepared, separated in 11% SDS-PAGE gels, and blotted on Immobilon-PVDF membrane (Merck Millipore, Billerica, MA) as previously described [11]. Membranes were incubated with antibodies against p53 (DO-7, BD Biosciences, Franklin Lakes, NJ; 1:1500), p21 (CP36/CP74, Merck Millipore, Billerica, MA; 1:1000), or GAPDH (14C10, Cell Signaling Technology, Danvers, MA; 1:3000). Secondary HRP-conjugated antibodies (Goat-anti mouse IgG and Goat-anti rabbit IgG, Merck Millipore, Billerica, MA; each 1:5000) and ECL chemiluminescent substrate were used for visualization at a ChemoCam Imager 3.2 (INTAS, Göttingen, Germany). Band densities were quantified using QuantityOne 4.6.7 (Bio-Rad, Hercules, CA). For control, always two values were used to reduce the overall scatter of the data. Densities of p53 and p21 bands were normalized to the expression of the housekeeping protein GAPDH and then corrected for the intensity of the total blot.

Specific Targeting of p53 by RNA Interference

Transfection of siRNA oligonucleotides was performed using Lipofectamine 2000 (Life Technologies, Carlsbad, CA) according to manufacturer's instructions. Briefly, cells were seeded into six-well plates and left overnight for adherence. Transfection of cells was carried out with 100 nM siRNA and 5 μl Lipofectamine for 4 hours in Opti-MEM (Life Technologies). The TP53 and nontargeting siRNA oligonucleotides (ON-Targetplus, SMARTpool) were purchased from Dharmacon (Horizon Discovery Group, Cambridge, UK).

Colony Formation Assay

Depending on cell line and treatment, 150-10,000 cells were seeded in 6-cm Petri dishes in triplicate. Depending on the therapeutic scheme (as indicated in the results section), cells were treated with BZM either directly after seeding or after attachment by a medium change. CDDP was applied directly into the growth medium at indicated time points. A final medium change including one third of conditioned growth medium (sterile filtrated supernatants of preserved growth medium of each cell line) was done to wash out BZM and/or CDDP. Cells were then allowed to grow for 7-22 days (depending on cell line and treatment). As treatments delayed colony formation, colonies were fixed at different time points aiming at equal colony sizes as compared to controls. After fixation (10% formaldehyde) and staining (0.1% crystal violet), colonies (>50 cells) were counted manually. Plating efficiencies (PEs) were calculated for each subgroup, and clonogenic surviving fractions (SFs) were calculated by normalization to untreated/unirradiated controls [24]. For each condition, at least three independent experiments were carried out.

Analysis of Cell-Cycle Distribution

Cells were fixed at indicated time points, and after staining with propidium iodide (PI), cell-cycle distribution was determined by a

LSR II flow cytometer (BD Biosciences, Franklin Lakes, NJ) and evaluated as previously described [11]. At least two independent experiments were carried out per cell line.

Detection of Apoptosis

Apoptotic cells were assessed using the Annexin V-FITC detection kit (Promokine, Heidelberg, Germany). Cells were detached from the surface, stained with Annexin V-FITC and PI according to the manufacturer's instructions, and analyzed as previously described [11]. Annexin V/FITC and PI double-positive cells were considered to be apoptotic, and their portion of all analyzed cells was calculated as previously described [25]. At least two independent experiments were carried out per cell line.

Statistical Analysis

If not otherwise indicated, results are presented as mean ± standard error of the mean (SEM) calculated from the independent experiments. Statistical significance was tested using the two-tailed Student's t test assuming a significance level of $P < .05$ (*), $P < .01$ (**), and $P < .001$ (***).

Results

BZM Restores p53/p21 Transactivation in HPV+ Cell Lines

To confirm the hypothesis of a functional restoration of p53 by BZM in HPV+ HNSCC cell lines, expressions of p53 and

Figure 1. Functional restoration of p53 in HPV+ cells after BZM treatment. Cells were treated with increasing BZM concentrations for 24 hours followed by protein analysis of p53 and p21 by Western blot. (A) Expression of p53 and p21 in UM-SCC-3 cells (HPV−) and UM-SCC-104 cells (HPV+). Level was normalized to the respective control values. (B) Average expression of p53 (left) and p21 (righ*t*) in three HPV− and four HPV+ cell lines. Mean values ± SEM for two independent experiments for each cell line after normalization to the respective GAPDH loading control.

downstream protein p21 were analyzed in four HPV+ and four HPV– cell lines using Western blot (Figure 1A; for detailed results, see Supplementary Figure S1). A low concentration of 10 nM BZM already led to a significant increase of p53 ($P = .0154$) and a strong induction of downstream protein p21 ($P = .0306$) in HPV+ cell lines (Figure 1B, black dots), which were further enhanced at a higher concentration of BZM. In contrast, in HPV– cell lines, expression of p53 was not affected, and only a marginal increase in p21 expression occurred at the highest concentration of BZM (Figure 1B, white circles).

BZM Enables IR-Induced p53/p21 Transactivation in HPV+ Cell Lines

Since p53 activation is critical for the cellular response on DNA damage caused by IR, we asked whether BZM also restores IR-induced p53 activation. The respective experiments were performed with one HPV+ (UM-SCC-47) and one HPV– (UM-SCC-3) cell line. For the HPV+ cell line, IR alone already led to a small increase of both p53 and p21 (Figure 2). However, especially for p21, the increase was much stronger when cells were pretreated with BZM with a further increase of about 35% after IR (Figure 2C, right columns). In contrast, for the HPV– cell line, IR slightly enhanced p53 expression, which was however abrogated by BZM. For p21, expression was even significantly decreased when BZM was followed by IR (Figure 2, B and C, left columns).

The increase of p21 expression in HPV+ cells after BZM alone but especially in combination with IR was shown to result from a functional p53 and not from an off-target effect of BZM on p21 because there was absolutely no increase of p21 when p53 was targeted by specific siRNA (Figure 2, D-F). Similar data were previously reported by others [19,20]. These data clearly demonstrate that BZM can be used to restore the IR-induced transactivation of p53/p21 in HPV+ cells.

BZM Induces Transient G1 Arrest in HPV+ Cell Lines upon Irradiation

Next, we analyzed the impact of BZM on cell-cycle regulation, which is an important mechanism depending on functional p53 especially when cells are exposed to IR. To this end, cell-cycle distribution was measured using flow cytometry (Figure 3, A) at 0, 7, and 24 hours after IR (4 Gy) with or without pretreatment with BZM (10 nM). The data summarized for all eight cell lines (Figure 3, B, C; for detailed results see Supplementary Figure S2) indicate that in HPV– cells, IR alone results in a moderate G2 arrest in contrast to a strong arrest detected for HPV+ cells, which is in line with previous data [8,9]. A G2 arrest was also detected after BZM alone, which, however, was clearly stronger for HPV– when compared to HPV+ cells (Figure 3, B, C). When BZM was given prior to IR, a further increase of cells in G2 phase was seen for HPV– cell strains when compared to IR alone (Figure 3, B, right columns). In contrast, for HPV+ cells, a strong increase in G2 phase was detected after IR alone but was clearly diminished with more cells arrested in G1 when cells were pretreated by BZM (Figure 3, C). These shifts in cell-cycle distribution demonstrate that HPV+ cells pretreated by BZM are able to induce a transient G1 arrest, thereby blocking cells to enter G2.

BZM Enhances the CDDP- and IR-Induced Apoptosis Only in HPV+ Cell Line

We also analyzed whether BZM will affect the induction of apoptosis, which is another critical mechanism regulated by p53. The
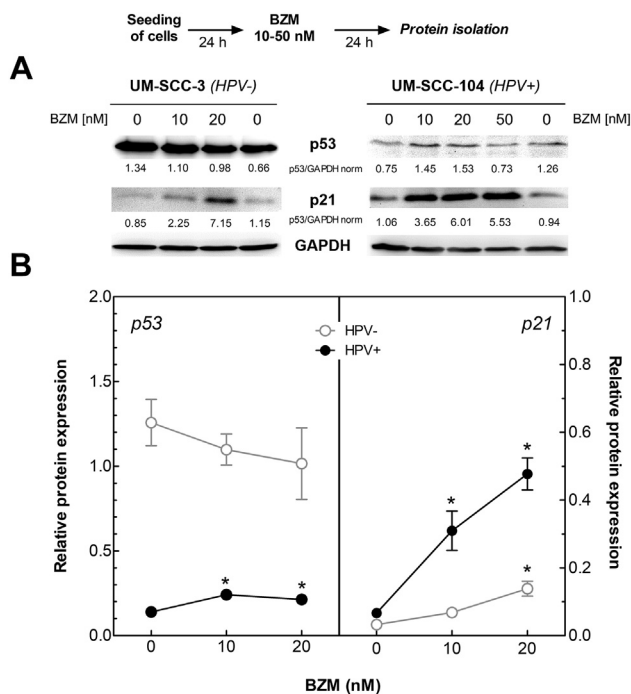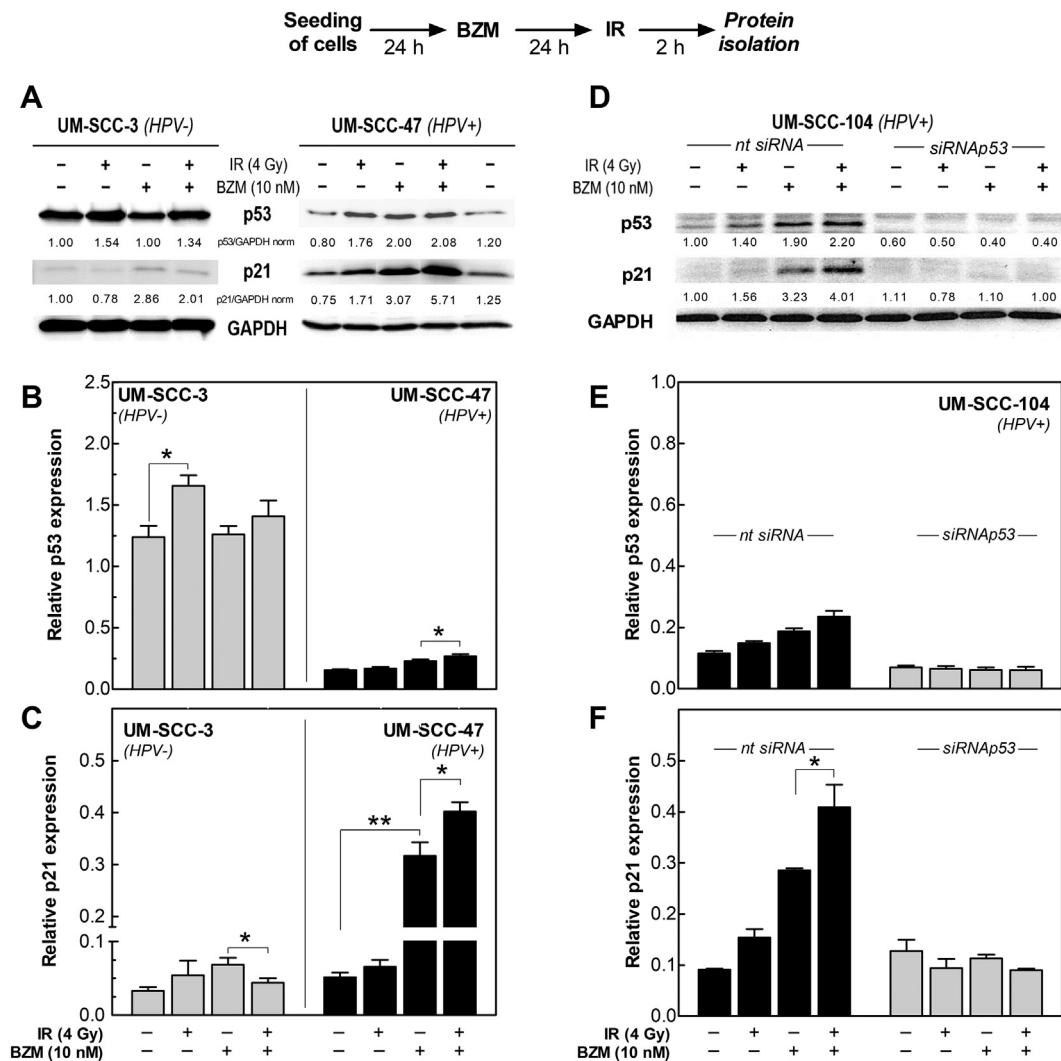
Figure 2. Functional restoration of IR-induced transactivation of p53 and p21 in HPV+ cells by BZM. Cells pretreated with 10 nM BZM for 24 hours were irradiated with 4 Gy followed by an incubation for 2 hours, and protein analysis was determined by Western blot. (A) Expression of p53 and p21 for UM-SCC-3 (HPV−) and UM-SCC-47 cells (HPV+). Level was normalized to the respective control value. (B, C) Relative expression of p53 (B) and p21 (C) after BZM ± IR in UM-SCC-3 and UM-SCC-47 cells. (D) Knockdown of p53 by targeting with specific siRNA in the HPV+ cell line UM-SCC-104. For targeting, cells were pretreated with TP53-specific or nontargeting siRNA for 24 hours. (E, F) Effect of knockdown of p53 on the expression of p53 and its transactivation of p21. Mean values ± SEM of three to five independent experiments after normalization to the respective GAPDH loading control.

induction of apoptosis was measured for one HPV− and one HPV+ cell line 24 and 48 hours after treatment with either IR or cisplatin (CDDP) alone or both treatments using Annexin V-FITC/PI-staining (Figure 4, A, B). In HPV− cells, only a minor induction of apoptosis (<5%) was seen after IR, CDDP, or its combination (Figure 4, C, light columns). This effect was not enhanced when cells were pretreated by BZM (Figure 4, C, dark columns).

For HPV+ cells, a low level of apoptosis was detected after IR alone (Figure 4, D, each first column). In contrast, a clear increase in apoptosis occurred when cells were treated by CDDP alone or in combination with IR, especially apparent 48 hours after treatment (Figure 4, D, seconds and third columns). Also, in HPV+ cells, BZM treatment alone led to induction of apoptosis. This was further enhanced when BZM was combined either with IR, CDDP, or both (Figure 4, D, dark columns). Overall, the increase in cell death was additive when compared to the effects seen without pretreatment with BZM. These data indicate that for HPV+ cells, BZM appears to

restore the p53-dependent apoptotic pathway especially observed after treatment including CDDP.

BZM Impairs Clonogenic Survival in Both HPV− and HPV+ Cell Lines

Next, the effect of BZM alone on colony formation was determined using two HPV− and two HPV+ cell lines, respectively. Surviving fractions of both HPV− and HPV+ cell lines were found to decrease with increasing concentration of BZM but with no obvious difference between the two groups (Figure 5).

BZM Affects Neither Radio- Nor Chemosensitivity of HPV− or HPV+ HNSCC Cell Lines

We also studied the effect of BZM on radio- and chemosensitivity using a concentration of 10 nM, which was shown to have an almost equal effect on survival in all four cell lines used (Figure 5). For the colony formation assay, different incubation times (10 to 21 days)
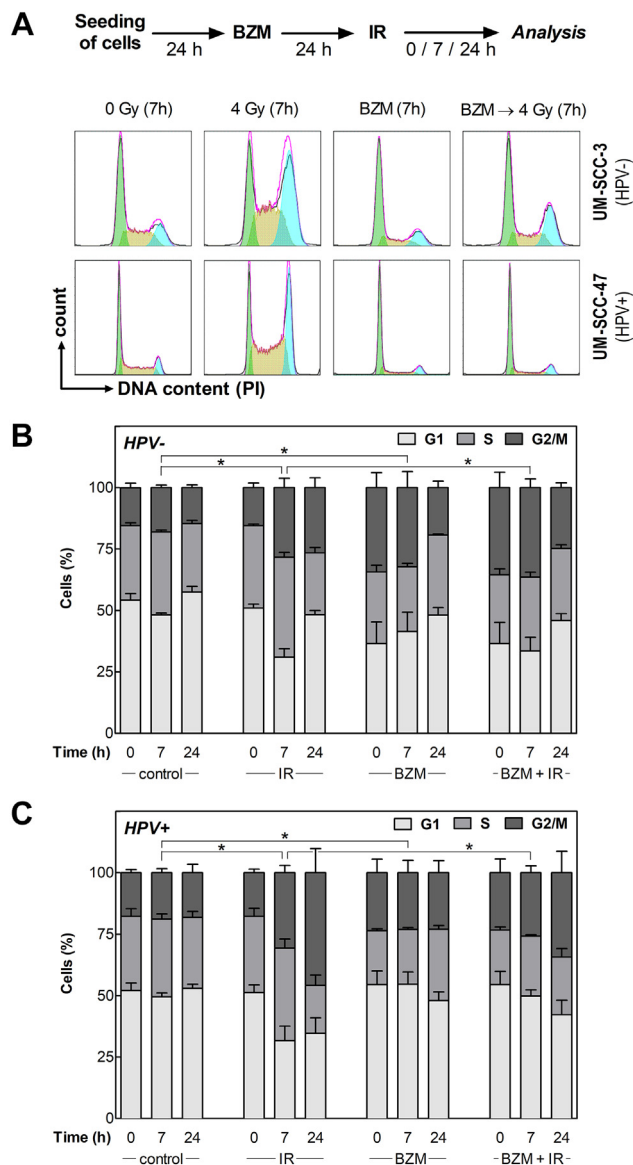
Figure 3. BZM restores transient radiation-induced G1-arrest in HPV+ cells. Cells pretreated with or without 10 nM BZM for 24 hours were irradiated with 0 or 4 Gy, and cell-cycle distribution was determined after an incubation for 0, 7, and 24 hours using flow cytometry. (A) DNA histograms of UM-SCC-3 (HPV−) and UM-SCC-47 (HPV+) cells at 7 hours after treatment. (B, C) Percentage of cells in G1, S, and G2/M phase as determined for three HPV− and four HPV+ cell lines 0, 7, and 24 hours after treatment. Data presented are mean values ± SEM of at least two independent experiments. Statistical differences were determined via χ^2 test.

had to be used in order to reach similar colony sizes (Figure 6A). The two HPV+ cell lines are significantly more radiosensitive when compared to the two HPV− cell lines as already shown previously [8,11] (Figure 6B, open symbols). Killing was not enhanced for either HPV− or HPV+ cells cell when cells were pretreated with BZM and cell survival was normalized to the effect of BZM alone (Figure 6B, closed symbols).

The effect of CDDP was studied for an incubation of 26 hours at concentrations up to 0.50 μM. The HPV+ cell line UM-SCC-47 was clearly more sensitive to CDDP as compared to the HPV− cell line

UM-SCC-3 as already reported previously [11]. Again, killing was not enhanced for either HPV− or HPV+ cells cell when cells were pretreated with BZM and cell survival was normalized to the effect of BZM alone (Figure 6C).

We finally tested the effect of BZM on the combined treatment of CDDP and IR using the two cell lines UM-SCC-3 (HPV−) and UM-SCC-47 (HPV+). For the two cell lines, different IR doses were chosen to adapt for divergence in sensitivity. For both cell lines, CDDP and BZM alone caused a slight reduction in surviving fraction, leading to an additive effect when combined as mentioned above (Figure 6, D and E, left columns). These effects are slightly stronger for HPV+ cells (Figure 6E). When IR was added to this combination, a further reduction of cell survival was seen, with the strongest reduction when all three treatments were applied. This reduction was much stronger for the HPV+ cell line as compared to the HPV− cell line. To test whether there are any synergistic effects, survival after combined treatments was normalized to the survival measured after IR alone (Figure 6, D and E, right columns). For these adjusted values, no significant differences were seen for either HPV− or HPV+ cells, indicating that the effect of the combined treatment with CDDP and IR is just additive irrespective of pretreatment with BZM or not. Overall, these data clearly demonstrate that BZM affects neither radio-/chemosensitivity nor the effect of a combined treatment with CDDP and IR.

Discussion

The aim of this study was to examine whether the proteasome inhibitor BZM can be used to prevent the degradation of p53 usually occurring in HPV+ HNSCC cells and whether this will restore the cellular stress dependent p53/p21 transactivation and respective downstream processes such as G1 arrest and apoptosis and thereby will enhance the cellular radio- and chemosensitivity.

The experiments were performed with four HPV+ and three HPV− HNSCC cell lines, previously reported to reflect typical features of these two entities with an enhanced sensitivity of HPV+ cells to both X-irradiation and CDDP [8–11].

For HPV+ but not for HPV− HNSCC cells, treatment with BZM was found to restore the transactivation of p53/p21 as previously described by others [19,20]. It is now shown here for the first time that this is also true for the radiation-induced transactivation, with a further increase of p21 in HPV+ cells when treated by BZM before exposure to IR (Figure 2).

We also observed that the restored transactivation of p53/p21 caused by BZM reactivates other important p53-dependent mechanisms such as G1 arrest and apoptosis (Figures 3 and 4). Treatment by BZM alone was found to induce a G2 arrest, which was slightly stronger for HPV− cells (Figure 3, B and C). The identical observation was made by Bullenkamp et al. [20] comparing five HPV+ with two HPV− cell lines. Most important, when BZM was given prior to IR in HPV+ cell lines, a transient G1 arrest was induced, causing a decrease in the strong G2 arrest normally seen in these cell lines (Figure 3C). This is a typical feature of tumor cells with a functional p53-dependent cell-cycle regulation after IR [26,27].

A clear difference between HPV− and HPV+ cells was also observed in respect to apoptosis. When treated by BZM alone, almost no apoptosis was seen for HPV− cells, in contrast to a clear induction in HPV+ cells (Figure 4) as was also found by others [20]. Solely for HPV+ cells, a further increase in apoptosis was obtained when BZM was given prior to IR, CDDP, or both of them (Figure 4D). This was
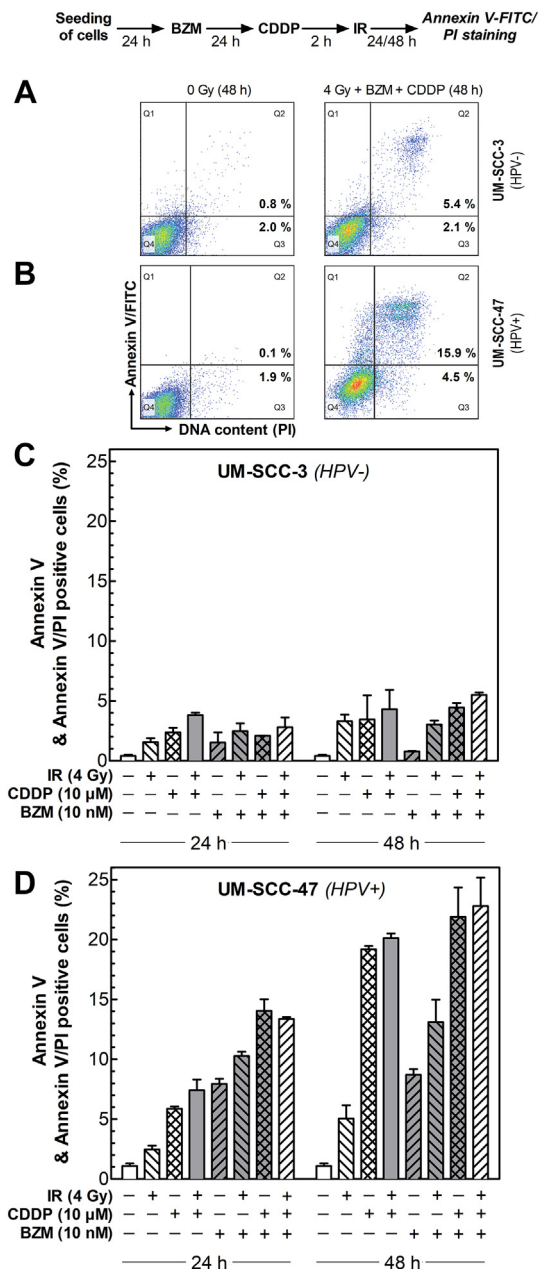
Figure 4. BZM restores damage-induced apoptosis in HPV+ cells. Cells treated with or without 10 nM BZM for 24 hours followed by an incubation with or without 10 μM CDDP for 2 hours were exposed to 0 or 4 Gy, and induction of apoptosis was determined 24 hours and 48 hours after IR using Annexin V-FITC/PI-staining. (A, B) Representative histograms of UM-SCC-3 (HPV−; A) and UM-SCC-47 (HPV+; B) cells 48 hours after indicated treatment. Fraction of cells in Q2 and Q3 was considered to represent apoptotic cells. (C) Fraction of apoptosis in the HPV− cell line UM-SCC-3; (D) fraction of apoptosis in the HPV+ cell line UM-SCC-47. Data presented are mean values ± SEM of at least two independent experiments.

Figure 5. BZM reduces cell survival in both HPV− and HPV+ cells. Cells were incubated with BZM for 24 hours at various concentrations (0-100 nM) before medium was changed, and cells were allowed to grow for colonies of at least 50 cells. Surviving fraction is shown as a function of BZM concentration. Data presented are mean values ± SEM of three independent experiments.

attributed to the restored p53/p21 transactivation achieved for HPV+ cells by BZM (Figures 1 and 2).

For the effect of BZM on cell survival, a huge variation was observed with no obvious difference between HPV− and HPV+ cell lines (Figure 5). 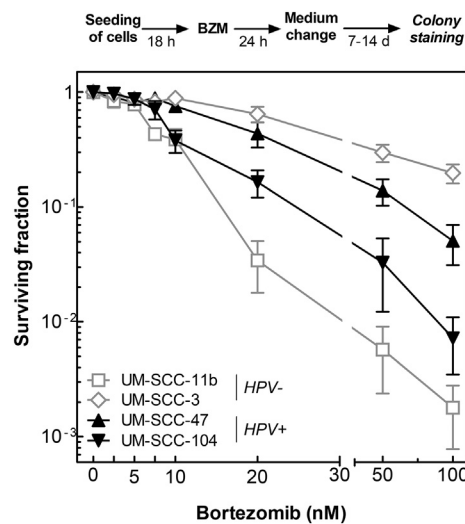Such a variation was previously also found for other cell lines and was suggested to result from different proteasome activities [28]. Our data also demonstrate that cell killing caused by BZM does not primarily result from apoptosis since the fraction of apoptotic cells was far below the total amount of cell killing achieved (Figures 4 and 5). Certainly, other cell death mechanisms are of relevance such as autophagy [29,30].

Pretreatment by BZM did not result in an enhanced radio- or chemosensitivity either for HPV+ or for HPV− cells. Even for the combination of IR and CDDP, solely additive effects were observed (Figure 6). In other reports, no or only a marginal radiosensitization was seen when BZM was combined with IR [31–34]. However, it should also be noted that, in these studies, sensitization was determined either via cell viability [32] or via colony assay, whereby all colonies were stained at the same time interval after treatment [31,33,34]. Hence, this protocol did not account for the different growth kinetics of the respective colonies as was done for here. Overall, these data indicate that BZM appears to increase the inhibitory effect of IR on cell growth but not on cell killing. This is in line with recent data obtained for xenograft tumors where the combination of BZM with IR was reported primarily to cause a strong growth retardation [35,36]. Such a reduction in cell growth was generally also seen when BZM was combined with CDDP [37–40].

After IR as well as CDDP, cell killing primarily results from chromosomal damage arising from either non- or misrepaired DNA double-strand breaks. But to a small extent, cell death may also result from a permanent G1 arrest or enhanced apoptosis [41]. However, even for an X-ray dose of 2 to 4 Gy, both of these effects on its own have to cause cell death in at least 20% of the population in order to have a significant impact on the total amount of cell killing [42]. This is far above the amounts seen here when BZM is combined with IR or CDDP. These data reveal that the restoration of p53/p21 transactivation and with that the induction of G1 arrest and apoptosis seen in HPV+ cells when treated by BZM are too small to cause a significant change in total cell killing when combined with IR, CDDP, or both.
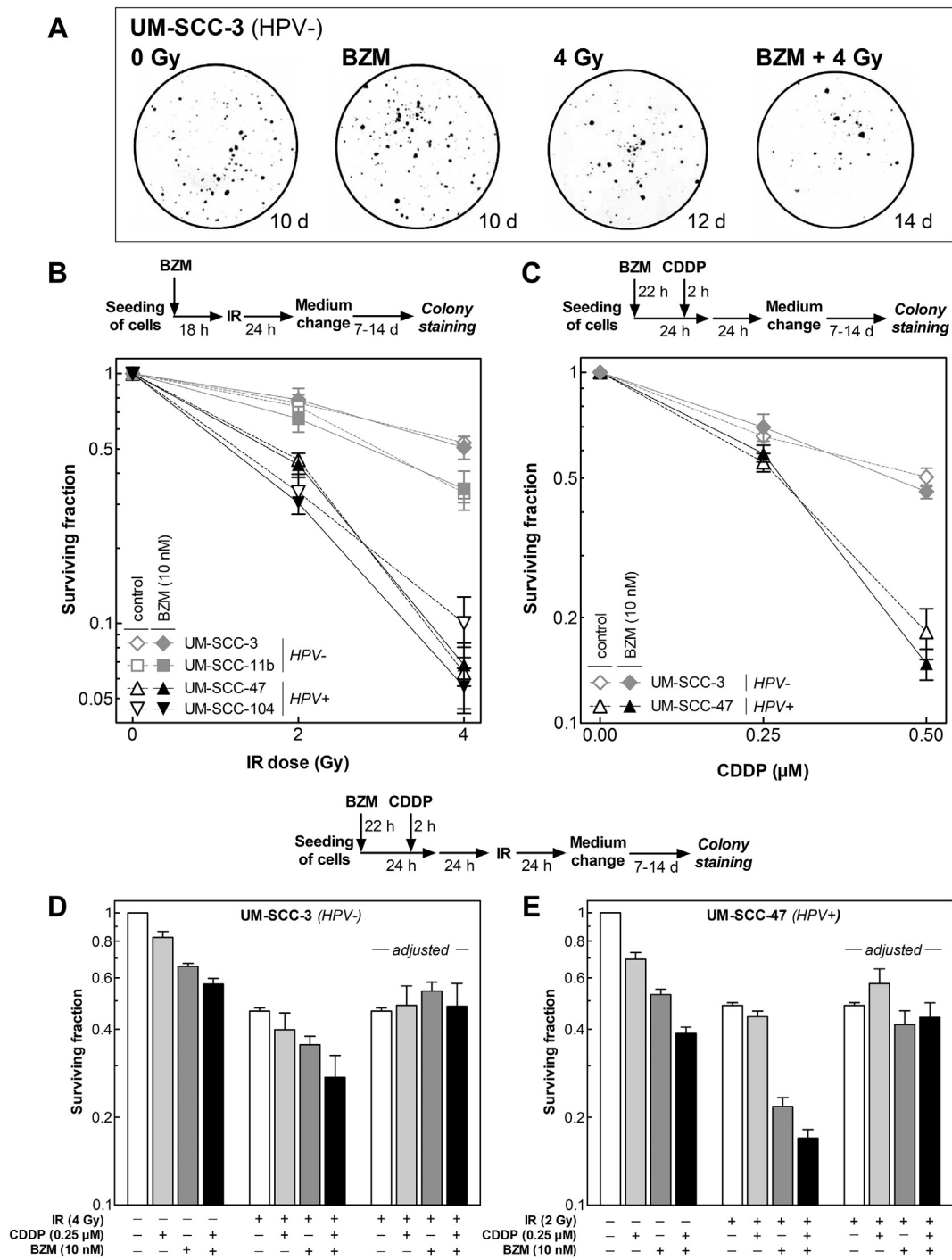
Figure 6. BZM does not affect radio- or chemosensitivity of HPV− and HPV+ HNSCC cell lines. (A, B) Effect on radiosensitivity was studied for cells which were incubated immediately after seeding with or without BZM for 24 hours before being exposed to X-rays followed by a further incubation for 24 hours. Thereafter, medium was changed, and cells were allowed to grow for colonies of about equal size. (C) Effect on chemosensitivity was studied by adding CDDP 22 hours after start of BZM treatment followed by a further incubation for 26 hours until medium was changed. (D, E) Effect of BZM on combined treatment was studied by adding CDDP 2 hours prior to irradiation. Data presented are mean values ± SEM of three independent experiments.

Overall, these data indicate that BZM combined with IR, CDDP, or both may not be an optimal regimen in the clinic as only additive effects were observed and thus no reduction in side effects can be achieved. In line with this, so far, BZM failed to show promising results in phase II clinical trials with solid tumors [43–45].

Conclusions

In conclusion, it was shown here for HPV+ HNSCC cells that although BZM is able to restore p53/p21-dependent pathways such as G1 arrest and apoptosis after IR and CDDP, no significant effect on radio- or chemosensitivity is achieved.

References

[1] Wittekindt C, Wagner S, Mayer CS, and Klussmann JP (2012). Basics of tumor development and importance of human papilloma virus (HPV) for head and neck cancer. *GMS Curr Top Otorhinolaryngol Head Neck Surg* **11**, 1–29.

[2] Sethi S, Ali-Fehmi R, Franceschi S, Struijk L, van Doorn LJ, Quint W, Albashiti B, Ibrahim M, and Kato I (2012). Characteristics and survival of head and neck cancer by HPV status: a cancer registry-based study. *Int J Cancer* **131**, 1179–1186.

[3] Mehanna H, Beech T, Nicholson T, El-Hariry I, McConkey C, Paleri V, and Roberts S (2013). Prevalence of human papillomavirus in oropharyngeal and nonoropharyngeal head and neck cancer–systematic review and meta-analysis of trends by time and region. *Head Neck* **35**, 747–755.

[4] Tinhofer I, Johrens K, Keilholz U, Kaufmann A, Lehmann A, Weichert W, Stenzinger A, Stromberger C, Klinghammer K, and Becker ET, et al (2015). Contribution of human papilloma virus to the incidence of squamous cell carcinoma of the head and neck in a European population with high smoking prevalence. *Eur J Cancer* **51**, 514–521.

[5] Ang KK, Harris J, Wheeler R, Weber R, Rosenthal DI, Nguyen-Tan PF, Westra WH, Chung CH, Jordan RC, and Lu C, et al (2010). Human papillomavirus and survival of patients with oropharyngeal cancer. *N Engl J Med* **363**, 24–35.

[6] National Comprehensive Cancer Network Guidelines. https://www.nccn.org/professionals/physician_gls/f_guidelines.asp#site, Accessed date: 17 November 2017.

[7] Mirghani H, Amen F, Blanchard P, Moreau F, Guigay J, Hartl DM, and Lacau St Guily J (2015). Treatment de-escalation in HPV-positive oropharyngeal carcinoma: ongoing trials, critical issues and perspectives. *Int J Cancer* **136**, 1494–1503.

[8] Arenz A, Ziemann F, Mayer C, Wittig A, Dreffke K, Preising S, Wagner S, Klussmann JP, Engenhart-Cabillic R, and Wittekindt C (2014). Increased radiosensitivity of HPV-positive head and neck cancer cell lines due to cell cycle dysregulation and induction of apoptosis. *Strahlenther Onkol* **190**, 839–846.

[9] Rieckmann T, Tribius S, Grob TJ, Meyer F, Busch CJ, Petersen C, Dikomey E, and Kriegs M (2013). HNSCC cell lines positive for HPV and p16 possess higher cellular radiosensitivity due to an impaired DSB repair capacity. *Radiother Oncol* **107**, 242–246.

[10] Busch CJ, Becker B, Kriegs M, Gatzemeier F, Kruger K, Mockelmann N, Fritz G, Petersen C, Knecht R, and Rothkamm K, et al (2016). Similar cisplatin sensitivity of HPV-positive and -negative HNSCC cell lines. *Oncotarget* **7**, 35832–35842.

[11] Ziemann F, Arenz A, Preising S, Wittekindt C, Klussmann JP, Engenhart-Cabillic R, and Wittig A (2015). Increased sensitivity of HPV-positive head and neck cancer cell lines to x-irradiation +/− Cisplatin due to decreased expression of E6 and E7 oncoproteins and enhanced apoptosis. *Am J Cancer Res* **5**, 1017–1031.

[12] Ziemann F, Seltzsam S, Dreffke K, Preising P, Arenz A, Subtil FSB, Rieckmann T, Engenhart-Cabillic R, Dikomey E, and Wittig A (2017). Roscovitine strongly enhances the effect of olaparib on radiosensitivity for HPV neg. but not for HPV pos. HNSCC cell lines. *Oncotarget* **8**(62), 105170–105183.

[13] Kimple RJ, Smith MA, Blitzer GC, Torres AD, Martin JA, Yang RZ, Peet CR, Lorenz LD, Nickel KP, and Klingelhutz AJ, et al (2013). Enhanced radiation sensitivity in HPV-positive head and neck cancer. *Cancer Res* **73**, 4791–4800.

[14] Cleary C, Leeman JE, Higginson DS, Katabi N, Sherman E, Morris L, McBride S, Lee N, and Riaz N (2016). Biological features of human papillomavirus-related head and neck cancers contributing to improved response. *Clin Oncol* **28**, 467–474.

[15] Riaz N, Morris LG, Lee W, and Chan TA (2014). Unraveling the molecular genetics of head and neck cancer through genome-wide approaches. *Genes Dis* **1**, 75–86.

[16] Mandinova A and Lee SW (2011). The p53 pathway as a target in cancer therapeutics: obstacles and promise. *Sci Transl Med* **3**, 1–7.

[17] Pellom Jr ST and Shanker A (2012). Development of proteasome inhibitors as therapeutic drugs. *J Clin Cell Immunol* (S5), 1–13.

[18] Chen D, Frezza M, Schmitt S, Kanwar J, and Dou QP (2011). Bortezomib as the first proteasome inhibitor anticancer drug: current status and future perspectives. *Curr Cancer Drug Targets* **11**, 239–253.

[19] Li C and Johnson DE (2013). Liberation of functional p53 by proteasome inhibition in human papilloma virus-positive head and neck squamous cell carcinoma cells promotes apoptosis and cell cycle arrest. *Cell Cycle* **12**, 923–934.

[20] Bullenkamp J, Raulf N, Ayaz B, Walczak H, Kulms D, Odell E, Thavaraj S, and Tavassoli M (2014). Bortezomib sensitises TRAIL-resistant HPV-positive head and neck cancer cells to TRAIL through a caspase-dependent, E6-independent mechanism. *Cell Death Dis* **5**, 1–9.

[21] Stone HB, Bernhard EJ, Coleman CN, Deye J, Capala J, Mitchell JB, and Brown JM (2016). Preclinical data on efficacy of 10 drug-radiation combinations: evaluations, concerns, and recommendations. *Transl Oncol* **9**, 46–56.

[22] Ballo H, Koldovsky P, Hoffmann T, Balz V, Hildebrandt B, Gerharz CD, and Bier H (1999). Establishment and characterization of four cell lines derived from human head and neck squamous cell carcinomas for an autologous tumor-fibroblast in vitro model. *Anticancer Res* **19**, 3827–3836.

[23] Mandic R, Schamberger CJ, Muller JF, Geyer M, Zhu L, Carey TE, Grenman R, Dunne AA, and Werner JA (2005). Reduced cisplatin sensitivity of head and neck squamous cell carcinoma cell lines correlates with mutations affecting the COOH-terminal nuclear localization signal of p53. *Clin Cancer Res* **11**, 6845–6852.

[24] Franken NA, Rodermond HM, Stap J, Haveman J, and van Bree C (2006). Clonogenic assay of cells in vitro. *Nat Protoc* **1**, 2315–2319.

[25] Greve B, Dreffke K, Rickinger A, Konemann S, Fritz E, Eckardt-Schupp F, Amler S, Sauerland C, Braselmann H, and Sauter W, et al (2009). Multicentric investigation of ionising radiation-induced cell death as a predictive parameter of individual radiosensitivity. *Apoptosis* **14**, 226–235.

[26] Olivier M, Bautista S, Valles H, and Theillet C (1998). Relaxed cell-cycle arrests and propagation of unrepaired chromosomal damage in cancer cell lines with wild-type p53. *Mol Carcinog* **23**, 1–12.

[27] Halacli SO, Canpinar H, Cimen E, and Sunguroglu A (2013). Effects of gamma irradiation on cell cycle, apoptosis and telomerase activity in p53 wild-type and deficient HCT116 colon cancer cell lines. *Oncol Lett* **6**, 807–810.

[28] Chen Z, Ricker JL, Malhotra PS, Nottingham L, Bagain L, Lee TL, Yeh NT, and Van Waes C (2008). Differential bortezomib sensitivity in head and neck cancer lines corresponds to proteasome, nuclear factor-kappaB and activator protein-1 related mechanisms. *Mol Cancer Ther* **7**, 1949–1960.

[29] Chang I and Wang CY (2016). Inhibition of HDAC6 protein enhances bortezomib-induced apoptosis in head and neck squamous cell carcinoma (HNSCC) by reducing autophagy. *J Biol Chem* **291**, 18199–18209.

[30] Li C and Johnson DE (2012). Bortezomib induces autophagy in head and neck squamous cell carcinoma cells via JNK activation. *Cancer Lett* **314**, 102–107.

[31] Cao W, Shiverick KT, Namiki K, Sakai Y, Porvasnik S, Urbanek C, and Rosser CJ (2008). Docetaxel and bortezomib downregulate Bcl-2 and sensitize PC-3-Bcl-2 expressing prostate cancer cells to irradiation. *World J Urol* **26**, 509–516.

[32] Goel A, Dispenzieri A, Greipp PR, Witzig TE, Mesa RA, and Russell SJ (2005). PS-341-mediated selective targeting of multiple myeloma cells by synergistic increase in ionizing radiation-induced apoptosis. *Exp Hematol* **33**, 784–795.

[33] Russo SM, Tepper JE, Baldwin Jr AS, Liu R, Adams J, Elliott P, and Cusack Jr JC (2001). Enhancement of radiosensitivity by proteasome inhibition: implications for a role of NF-kappaB. *Int J Radiat Oncol Biol Phys* **50**, 183–193.

[34] Weber CN, Cerniglia GJ, Maity A, and Gupta AK (2007). Bortezomib sensitizes human head and neck carcinoma cells SQ20B to radiation. *Cancer Biol Ther* **6**, 156–159.

[35] Huang CY, Wei CC, Chen KC, Chen HJ, Cheng AL, and Chen KF (2012). Bortezomib enhances radiation-induced apoptosis in solid tumors by inhibiting CIP2A. *Cancer Lett* **317**, 9–15.

[36] Tamatani T, Takamaru N, Hara K, Kinouchi M, Kuribayashi N, Ohe G, Uchida D, Fujisawa K, Nagai H, and Miyamoto Y (2013). Bortezomib-enhanced radiosensitization through the suppression of radiation-induced nuclear factor-kappaB activity in human oral cancer cells. *Int J Oncol* **42**, 935–944.

[37] Konac E, Varol N, Kiliccioglu I, and Bilen CY (2015). Synergistic effects of cisplatin and proteasome inhibitor bortezomib on human bladder cancer cells. *Oncol Lett* **10**, 560–564.

[38] Li C, Li R, Grandis JR, and Johnson DE (2008). Bortezomib induces apoptosis via Bim and Bik up-regulation and synergizes with cisplatin in the killing of head and neck squamous cell carcinoma cells. *Mol Cancer Ther* **7**, 1647–1655.

[39] Miyamoto Y, Nakagawa S, Wada-Hiraike O, Seiki T, Tanikawa M, Hiraike H, Sone K, Nagasaka K, Oda K, and Kawana K, et al (2013). Sequential effects of the proteasome inhibitor bortezomib and chemotherapeutic agents in uterine cervical cancer cell lines. *Oncol Rep* **29**, 51–57.

[40] Wagenblast J, Hambek M, Baghi M, Gstottner W, Strebhardt K, Ackermann H, and Knecht R (2008). Antiproliferative activity of bortezomib alone and in combination with cisplatin or docetaxel in head and neck squamous cell carcinoma cell lines. *J Cancer Res Clin Oncol* **134**, 323–330.

[41] Borgmann K, Dede M, Wrona A, Brammer I, Overgaard J, and Dikomey E (2004). For X-irradiated normal human fibroblasts, only half of cell inactivation results from chromosomal damage. *Int J Radiat Oncol Biol Phys* **58**, 445–452.

[42] Kriegs M, Gurtner K, Can Y, Brammer I, Rieckmann T, Oertel R, Wysocki M, Dorniok F, Gal A, and Grob TJ, et al (2015). Radiosensitization of NSCLC cells by EGFR inhibition is the result of an enhanced p53-dependent G1 arrest. *Radiother Oncol* **115**, 120–127.

[43] Zhao Y, Foster NR, Meyers JP, Thomas SP, Northfelt DW, Rowland Jr KM, Mattar BI, Johnson DB, Molina JR, and Mandrekar SJ, et al (2015). A phase I/II study of bortezomib in combination with paclitaxel, carboplatin, and concurrent thoracic radiation therapy for non-small-cell lung cancer: North Central Cancer Treatment Group (NCCTG)-N0321. *J Thorac Oncol* **10**, 172–180.

[44] O'Neil BH, Raftery L, Calvo BF, Chakravarthy AB, Ivanova A, Myers MO, Kim HJ, Chan E, Wise PE, and Caskey LS, et al (2010). A phase I study of bortezomib in combination with standard 5-fluorouracil and external-beam radiation therapy for the treatment of locally advanced or metastatic rectal cancer. *Clin Colorectal Cancer* **9**, 119–125.

[45] Argiris A, Duffy AG, Kummar S, Simone NL, Arai Y, Kim SW, Rudy SF, Kannabiran VR, Yang X, and Jang M, et al (2011). Early tumor progression associated with enhanced EGFR signaling with bortezomib, cetuximab, and radiotherapy for head and neck cancer. *Clin Cancer Res* **17**, 5755–5764.